Modelling Approach to Predict the RFID Read Rates on a Complex Set of Materials

Renuka Nalinggam [1] and Widad Ismail [2]

[1] Faculty of Engineering & Information Technology, Southern University College
Jalan Selatan Utama, Off Jalan Skudai, 81300 Skudai, Johor
renukanalinggam@sc.edu.my

[2] Auto ID Laboratory, School of Electrical and Electronic Engineering, Universiti Sains Malaysia (USM)
Engineering Campus, 14300 Nibong Tebal, Pulau Pinang, Malaysia
eewidad@usm.my

Abstract ─ This research provides a platform to prove the potential of radio-frequency identification (RFID) technology for use in hypermarket payment systems. A 2.54 GHz ZigBee-based embedded passive and active RFID (EPARFID) system was developed to obtain experimental data and subsequently analyze passive RFID characteristics. A read rate prediction model based on materials permittivity value is proposed. Combining experimental data with analytical electromagnetic models improved the extrapolation of RFID read rates in a given environment. The modelling approach is a step toward the development of a robust methodology to predict RFID read rates on a complex set of materials. Results obtained from the proposed prediction modelling of read rates based on the Friis free space equation by quantifying uncertainties provide new insights into the nature of tag read rates.

Index Terms ─ Relative permittivity, RFID modelling, RFID on complex materials, RFID read rate prediction.

I. INTRODUCTION

Radio-frequency identification (RFID) technology is applied to the location and tracking of objects. Thus, RFIDs are used in a wide range of industrial fields, such as factory automation, distributed and process control, traceability management, supply chain management, real-time monitoring of health, and radiation check [1]. RFID has been recently applied to many location identification systems to detect the presence of tagged objects and/or people. Localization using an RFID reader is important to provide improved and efficient context-aware services [1]. Most studies related to RFID focus on the application of RFID technology to provide tag identification and for tracking purposes only [2].

Considering that studies focus on the development of a prototype to be applied at item-level tagging for retail applications, researchers have presented several comparisons based on previous literature findings on the RFID system application to retail tracking systems. This comparison review aims to determine the accurate problem encountered in a retail platform. Moreover, the review will contribute to the research by identifying priority factors that require attention and providing potential solutions for problems.

From the reviews [3-6], researchers anticipate and highly recommend the standardized RFID system for global application and tag performance (despite the material surface) as a highly recommended concern. Thus, the current research was conducted to offer potential solution for the issues highlighted in the review.

RFID is related to the procedure of transmitting and recognizing object in the form of a unique serial number through the RF wave. The range of an RFID system is determined by the power emitted by the reader antenna, the power available within the tag, the type of passive tag, the orientation of the antenna and the tag, and the surface of the material on which the tag is placed. The power available within the tag received from the reader will be converted into energy to activate the chip inside the tag. Tagged surface materials also play a vital role, because they may influence RFID performance in terms of distance and read rate because of the effect of various parameters, such as dielectric constant, radiation efficiency, and radiation impedance caused by the diversity of material properties [7]. Radio-frequency (RF) signals contain information that has been modulated from RF waves. The behavior of RF signals can be detected and predicted. They can be interfaced with other signals and react differently to various materials. Typical material reactions toward RF signals are reflection, absorption, and attenuation, which reduce the reliability and performance of RFID systems in terms of tag detection [8]. This phenomenon limits the implementation of RFID systems on material-related

Submitted On: July 9, 2018
Accepted On: March 24, 2019

applications. Different materials produce varying read rates in an RFID system.

Performing experiments on material reaction using the preferred materials is a highly effective means to obtain the read rate of each type of material. However, measuring the read rates of all materials available in hypermarkets is economically not feasible and time consuming. The lack of measured read rate data on a material of interest results in the development of power prediction models. Many models are available for predicting tag read rates [9-13].

Most models are developed by focusing only on available power in tags, reader-transmitted power, antenna gain, and distance estimation. To demonstrate the eligibility of RFID technology for hypermarket application, tag surface material parameters are the factors considered in a prediction model. Although numerous researchers have developed prediction models [9-13] (as summarized in Table 1) that can be used to predict tag read rates, uncertainties remain in selecting a suitable model that can be applied to research. Thus, real-time measurement results should be compared with a suitable prediction model to validate its accuracy. Each prediction model has advantages and limitations. A power prediction model should be modified on the basis of limitations observed in existing models. Therefore, determination of measured experimental data is an important requirement to select an optimum read rate prediction model.

The current research aims to develop a multi-band RFID by embedding the passive and active RFIDs as a single system platform (EPARFID), investigate the eligibility of the developed EPARFID system in hypermarkets' checkout payment system, and propose a suitable modified RFID read rate prediction model to predict tag read rate reliability on the basis of the materials' relative permittivity. RFID (passive system) and WSN are integrated into an active RFID (EPARFID) system to determine the existence of a significant improvement in monitoring. This process will provide an opportunity for the RFID technology to work in a wireless platform, with a long range, wide area, and in multi-hop communication [6], as shown in Fig. 1.

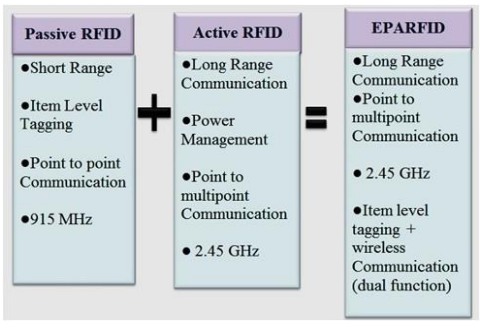

Fig. 1. Passive and active (EPARFID) system layout.

Table 1: Review on available RFID read rate prediction models

Research Title	Input Parameters	Outcome	Application
[9]	P_r, G_r, G_t, λ and d	Undefined	Experimental data presentation on critical aspects of the UHF RFID systems
[10]	Reader: P_r, P_T, G_r, G_T, and radar cross section of the RF tag	To quantify the effects on RF tag material attachment	RF tag designer
[11]	Impedance matching, coupling coefficient, and impedance-matching coefficient	To obtain power observed by the tag chip	Item-level tagging
[12]	EIRP, G_{Reader}, S_{11}, S_{22}, S_{21}, LF, R_2 and X_2	To predict power transmitted to the chip	To predict electromagnetic compatibility performance in complex aeronautic areas
[13]	Zc (chip input impedance) and Za (antenna input impedance)	To predict impedance matching between the reader antenna and the tag chip	Compact and low-profile tag for metal application
Proposed EPARFID System	P_r, G_r, G_t, ε_r, λ, and d	RFID read rate prediction based on dielectric permittivity	RFID system developers for hypermarket or supply chain application

The passive and active portions in the proposed EPARFID system are non-separable. They involve three main segments, namely, passive tag (tag on materials), active tag (payment counter), and active reader (display). The system must perform two types of communications to display the data. The first part of communication occurs between the passive and active tags. The second part of communication occurs between the active tag and the active reader. Then, the data can be displayed. During the first-part communication, passive RFID-related characteristics, such as distance between passive tag and reader, passive tag on materials, and passive tag surface are found. During the second part of the communication,

active RFID-related characteristics, such as multi-hop, throughput, self-healing, and latency were discovered.

Therefore, the actual experiments were conducted to identify the abovementioned characteristics and provide standard guidelines for the EPARFID system. On the basis of these characteristics, the power prediction model was modified. Moreover, the result was compared with the actual experiment data to determine efficiency. The power prediction model parameters focused on the passive RFID characteristics and not the active RFID. As stated previously, the segments in the EPARFID system are non-separable portions, and the research focused on hypermarket application. Thus, passive RFID characteristic parameters, such as placement of passive tag on materials, the materials' permittivity value, and the distance between passive tag and reader, become the main concerns in model modification. This finding is explained by the fact that the first segment communication (Passive RFID) of the EPARFID system affects the second segment communication (Active RFID) of the system.

This work aims to provide fundamental data on the design of experiments that involve a complete analysis related to standard packaging materials available in hypermarkets.

Many researchers [3, 4, 13-16] acknowledged that dielectric materials provide significant effects on RFID reading performance. Their studies are emphasized on tag surface dielectric permittivity value only. Tag surface dielectric permittivity value alone is insufficient for this research as packaging materials in retails contain a certain filling. Therefore, emphasis on the permittivity value of the surface (metal, glass, plastic, and cardboard) and the subsurface (water, powder, and paste) of packaging materials is an added novelty for this research. Table 2 presents the relative permittivity values of the surface and subsurface of the materials involved in this research.

In practical applications, quantities such as polarizabilities and scattered thicknesses are not the most convenient to use. Instead, it is preferable to play with the permittivity of the components of the mixture. The most common mixing rule is the *Maxwell Garnett* formula, which is written explicitly for the effective permittivity [17].

The mixing equation for general thin mixture is as follows:

$$\varepsilon_{eff} = \varepsilon_e + 3f\varepsilon_e \frac{\varepsilon_i - \varepsilon_e}{\varepsilon_i - 2\varepsilon_e}, \quad (1)$$

where f is the ratio between $\frac{\varepsilon_i}{\varepsilon_e}$, for the Maxwell Garnett prediction of the effective permittivity of a mixture with inclusions of permittivity, and ε_i in a background medium of permittivity, ε_e. Therefore, ε_i and ε_e are defined as subsurface and surface relative permittivities, respectively [17].

II. MODIFICATION OF A POWER PREDICTION MODEL

A simple propagation model is used as a reference to predict passive tag read rates at difference distances and tag surfaces. The modelling approach is one step toward the development of a robust methodology for predicting RFID read rates on a complex set of materials. Thus, a power prediction model equation, namely, equation (2), is modified to determine the power absorbed by an RFID tag chip. Simple dipole-like antennas are utilized in all ultra-high frequency (UHF) passive tags. These antennas can be easily fabricated, and their size is controlled due to the radiation wavelength. Efficient power delivery to the chip by the power available at the tag antenna will maximize tag performance [18].

In general, the power P_t received and available at the tag antenna output connector can be generally determined, as follows:

$$P_{t} = P_r . \rho . C, \quad (2)$$

where P_r is the power at the input connector of the reader antenna, ρ is the impedance-matching coefficient between the reader and its antenna, and C is the coupling coefficient between the reader's and tag's antennas [11].

In UHF RFID systems, critical conditions are met far from the reader's antenna, in which the maintenance of high-power levels is important to activate passive tags and ensure an observable backscattered signal [14]. Such configuration allows UHF systems to operate under far-field conditions at the reader and tag sides. Under these conditions, the radiated electric and magnetic fields propagate as plane waves perpendicular to one another and to the wave propagation direction.

When an ideal matching between the reader and its antenna (ρ = 1) is considered, P_t in Equation (2) (unit: dBm) changes into the following:

$$P_{t,dBm} = P_{r,dBm} + G_{t,dB} + G_{r,dB} + \rho_{dB} + 20.\log_{10}\left(\frac{\lambda}{4\pi d}\right), \quad (3)$$

where G_r and G_t are the antenna gains of the reader and tag, respectively; ρ is the polarization mismatch coefficient between these gains; and d is the distance between the reader's antenna, which is the attenuation caused by propagation in space.

However, the tag antenna designed for a particular application, such as for mounting on a metallic surface, may be incompatible with a different surface, even that within the same class of products. This phenomenon is explained by the limit of the antenna's bandwidth, which leads to detuning when placed on a material with dielectric properties outside the design range.

In real-life applications, performance may deteriorate closer to the reader's antenna. In general, inferior performance can be expected with respect to distance, because parasitic effects (i.e., relative permittivity)

influence system behavior. Accordingly, this research focuses on the influence of dielectric permittivity on RFID read range performance [3]. Thus, the dielectric permittivity ($\mathcal{E}_r$) of tagged surfaces is a crucial parameter that should be included in Equation (3). When the wave penetrates the permittivity medium with relative permittivity $\mathcal{E}_r$, the wavelength becomes the following:

$$\lambda = \frac{1}{f\sqrt{\mu_0 \varepsilon_0 \varepsilon_r}}, \quad (4)$$

where $\mathcal{E}_r$ is the relative permittivity value of the medium [18]. Table 2 provides the relative permittivity values of the materials involved in this research. This research focuses on the tag surface and subsurface of materials. Thus, Fig. 2 illustrates the emphasized tag surface and subsurface.

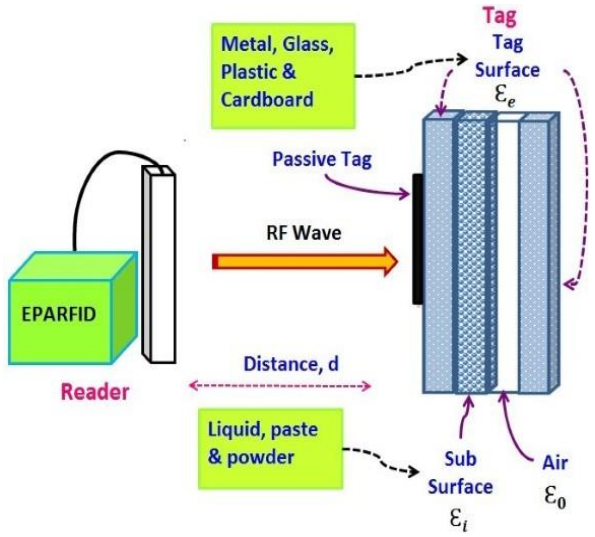

Fig. 2. Illustration of the emphasized tag surface and subsurface emphasized.

Tag surface permittivity and filling permittivity are combined based on (1). Tag surface (e.g., metal, glass, plastic, and cardboard) permittivity value is defined as environment permittivity $\mathcal{E}_e$. By contrast, the content of respective materials (e.g., water, paste, detergent, and powder) is assumed as inclusion permittivity $\mathcal{E}_i$. The value of f obtained for all the combinations is lower than 1. Hence, the respective material permittivity value is substituted into (1). Table 3 presents the $\mathcal{E}_{eff}$ value substituted into (4) as the $\mathcal{E}_r$ value based on the respective material's surface and subsurface values and the respective material's effective permittivity values. The terms provided in Table 3 are the small form of the standard packaging material's surface and subsurface, that is, MLA means the following: (M) stands for metal surface, (L) stands for liquid subsurface, and (A) is the tag type.

Table 2: Permittivity of respective materials

Materials	Dielectric Permittivity, $\mathcal{E}_r$
Metal (M)	9.7
Plastic (P)	2.5
Glass (G)	8
Cardboard (C)	2
Air	1
Water/Liquid (L)	78
Powder (P)	3.5
Paste (D)	50

Table 3: Absolute permittivity values of material combination in the research

Terms	Material Surface (Environment Permittivity, εe)	Material Subsurface (Inclusion Permittivity, εi)	εeff
MLA	9.7	78	66.01
MPA		3.5	6.50
MDA		50	39.31
GLA	8	78	67.76
GPA		3.5	4.41
GDA		50	50.00
PLA	2.5	78	74.43
PPA		3.5	2.71
PDA		50	50.00
CLA	2	78	75.11
CPA		3.5	2.50
CDA		50	40.67

A tag is assumed to be readable if P_t exceeds a power threshold P_{th}. When $P_t < P_{th}$, the available power is insufficient for the tag to respond [9]. The following is a summary of the main parameters. Their values are used to check the power absorbed by the tag at 0.3 m. In this scenario, the tag is placed on a cardboard filled with powder. P_r = 30 dBm; G_r = 8 dB; G_t = 2.15 dB; ε_{eff} = 2.50; λ = 0.2073 m; d = 0.3 m.

When the preceding parameters are substituted into (3), the prediction of the power absorbed by the tag is 11.981 dBm. The P_t value is higher than P_{th} = −12 dBm. Thus, the tag is assumed to be readable. The method is repeated at different distances of 0.5 and 0.7 m, as shown in Table 4. Figure 3 displays the layout design of the measurement setup of the embedded passive and active RFID (EPARFID) system with three different distances.

III. RESULT AND ANALYSIS OF THE MODIFIED POWER PREDICTION MODEL

Variations between 0 and 0.3 m, 0.3 and 0.5 m, and 0.5 and 0.7 m were implemented to obtain 10 average values of the tags that responded and those that did not respond. On the basis of the average value of the linear

equation, the respective distance was obtained as follows [19]:

$$P_t = 0.9478\varepsilon_{eff} + 9.5412 \text{ at } 0.3 \text{ m}, \quad (5)$$
$$P_t = 0.9478\varepsilon_{eff} - 10.549 \text{ at } 0.5 \text{ m}, \quad (6)$$
$$P_t = 0.9478\varepsilon_{eff} - 40.459 \text{ at } 0.7 \text{ m}. \quad (7)$$

Table 4: Received power level of the tag with respect to the effective permittivity ε_{eff} for the distances of 0.3, 0.5, and 0.7 m

Surface + Subsurface	ε_{eff}	Non-Line-of-Sight Transmission		
		P_t (dBm)		
		0.3 m	0.5 m	0.7 m
CLA	75.11	−2.860	−5.782	−13.488
PLA	74.43	−2.820	−5.743	−13.449
GLA	67.76	−2.413	−5.335	−13.041
MLA	66.01	−2.299	−5.221	−12.928
CDA	47.18	−0.840	−3.763	−11.469
PDA	46.52	−0.779	−3.702	−11.408
GDA	40.67	−0.196	−3.118	−10.824
MDA	39.31	−0.048	−2.970	−10.677
MPA	6.50	7.768	4.846	−2.861
GPA	4.41	9.453	6.530	−1.176
PPA	2.71	11.567	8.645	0.939
CPA	2.50	11.918	8.995	1.289

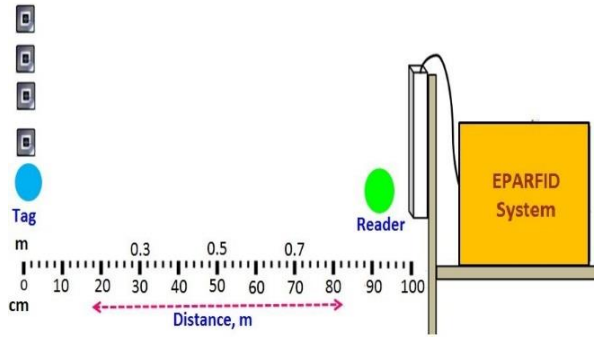

Fig. 3. Measurement setup of the EPARFID system with three different distances.

On the basis of Equations (5), (6), and (7), the graphs of the received power level of the tag with respect to the relative permittivity are plotted for the distances of 0.3, 0.5, and 0.7 m in Figs. 4 to 6. As shown in Fig. 4, the received power of the tag at all the relative permittivity values is higher than −12 dBm, which indicates that 100% of the tag detection is achieved at 0.3 m. As shown in Fig. 5, most of the values are maintained at a level higher than the threshold value. By contrast, Fig. 6 shows that the tag with a dielectric permittivity value of over 50 is not detected at 0.7 m.

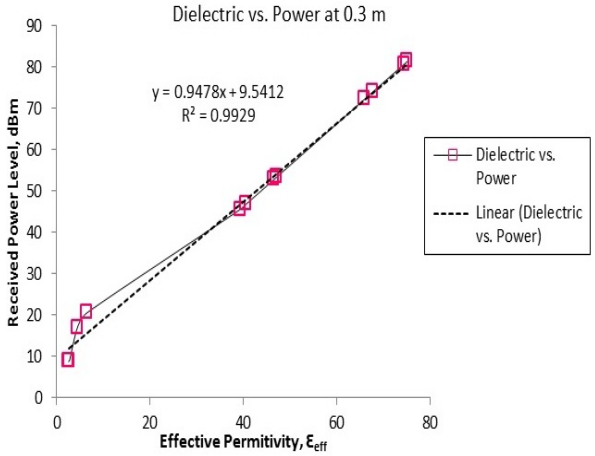

Fig. 4. Dielectric vs. received power of the tag at 0.3 m.

Ten average values obtained from the EPARFID system and predicted by the proposed model were compared at distances of 0.3, 0.5, and 0.7 m. In terms of detection percentage, the EPARFID system and the modelling achieved 100% at 0.3 m. At 0.5 m, the detection percentages achieved by the EPARFID system and the modelling are 90% and 96.8%, respectively. The detection achieved at 0.7 m by the EPARFID system is 65.5%, and that of the modelling is 68.7%. The modelling achieves 0 root mean square (RMS) value at an ideal distance, and the value increases with increasing distance. At low RMS value, the performance improves. The distance between the tag and the reader significantly affects system performance. Thus, higher RMS value is obtained at a longer distance.

The tag read rate reliability percentages of the EPARFID system and the proposed model are calculated as follows:

$$Read\ Rate\ Reliability\ (\%) = \frac{Responded\ Tag}{Total\ Tag} \times 100\%. \quad (8)$$

The responded tag in (8) indicates the total number of tags that successfully responded during the experiment. Total tag denotes the number of experiment repetitions. All the experiments were repeated 10 times to obtain 10 average data for analysis.

At 0.3 m, the modelling and EPARFID system achieved 100% tag detection. Thus, 0.3 m is the optimum distance between the tag and the reader regardless of the tag surface and orientation, as shown in Fig. 7. Moreover, the modelling and EPARFID system maintained a 100% detection percentage for tag surfaces with an effective permittivity of 2.5–20 at 0.5 m. The model and EPARFID system achieved 90% detection percentage for an effective permittivity of 20–60 and 80% for an effective permittivity of 60 and higher, as shown in Fig. 8. At 0.7 m, the EPARFID system

maintained 70% detection percentage for tag surfaces with an effective permittivity of 2.5–60. Then, the percentage dropped to 60% and 50% for effective permittivity of 60–70 and 70 and higher, respectively. By contrast, the proposed model achieved 80% detection percentage for an effective permittivity of 2.5–10, 70% for an effective permittivity of 40–60, and 60% for an effective permittivity of 60 and higher as shown in Fig. 9.

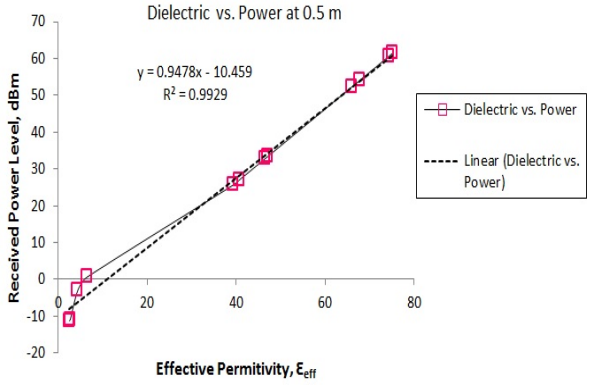

Fig. 5. Dielectric vs. received power of the tag at 0.5 m.

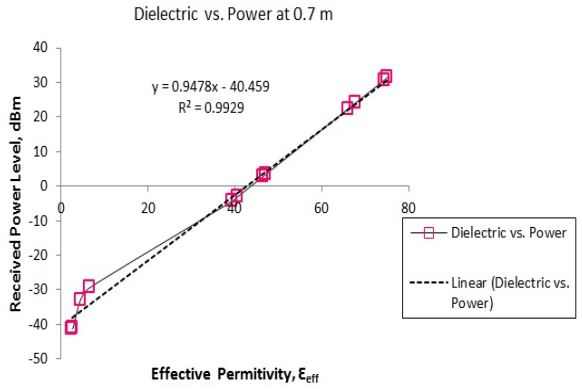

Fig. 6. Dielectric vs. received power of the tag at 0.7 m.

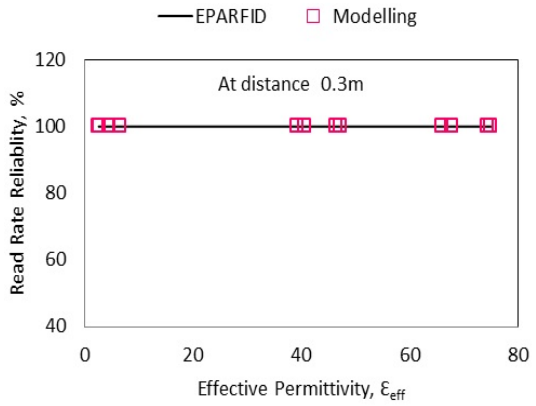

Fig. 7. EPARFID system vs. proposed model at 0.3 m.

The analysis demonstrates that the presence of dielectric materials on the tag surface can damage RF signal strength and reduce its read range performance, because the tag no longer works in free space. A tag antenna designed for a particular application, such as mounting on a metallic surface, may be incompatible with a different surface, even that belonging to the same class of products. This phenomenon is due to the bandwidth limit of the antenna. Detuning occurs when the tag is placed on a material with dielectric properties outside the designed range. Moreover, the thickness of a material affects the tuning of dielectric media with medium to high permittivity and varying thickness values. Therefore, fixing the distance between the tag and the reader can be a potential solution for selecting a standard RFID system and tag that can be applied to different materials. The analysis proves that the distance between the reader and the tag is a critical aspect that requires consideration during system performance. The optimum performance of the proposed system can be achieved by maintaining the distance between the tag and the reader at 0.3 m. As the distance between the tag and the reader increases, the performance percentage of the tag decreases or the tag becomes unreadable.

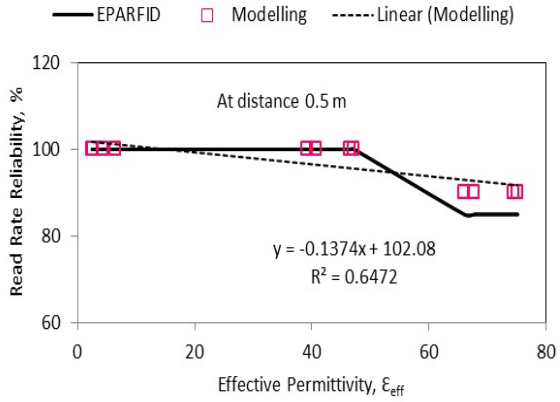

Fig. 8. EPARFID system vs. proposed model at 0.5 m.

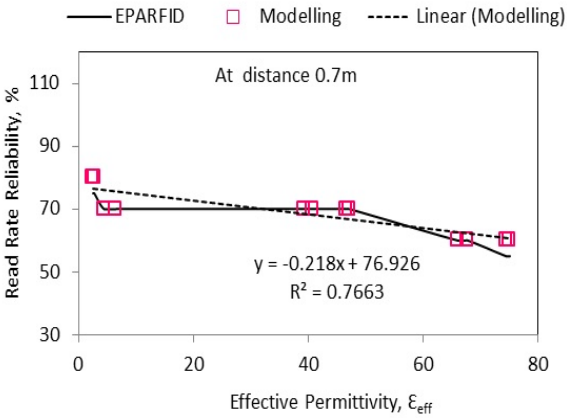

Fig. 9. EPARFID systems vs. proposed model at 0.7 m.

The analysis indicates that the power data predicted by the proposed model closely follow the experimental data obtained from the EPARFID system experiments, particularly at the ideal distance of 0.3 m. The confirmation of the closeness of the proposed model verified that the EPARFID system's experimental data can be observed at 0.5 and 0.7 m.

IV. CONCLUSION

This research successfully validates that RFID technology does not require line-of-sight transmission to detect passive tags. The tag detection results are precise regardless of orientation if the distance between the passive tag and the reader does not exceed 0.3 m, depending on the signal quality of the reader. The relative dielectric permittivity of the materials used in the experiment significantly affects EPARFID performance. Materials with low relative permittivity demonstrate consistent performance than materials with high relative permittivity. Perceiving trends on how read rate probabilities vary with distance, power level, and tag surface relative permittivity for a set of materials is remarkable. Combining experimental data with analytical electromagnetic models improves the extrapolation of RFID read rates in a given environment. The results obtained from the proposed prediction model of read rate based on Friis free space equation by quantifying uncertainties provide new insights into the nature of tag read rates. Furthermore, confirming the closeness of the results of the proposed modelling approach to the EPARFID system experimental data establishes the validity of the proposed modelling approach. In conclusion, the findings and discussions presented by this research possibly serve as a guideline for improving feasibility and eligibility of the EPARFID system development and framework and create awareness for retail application on item-level tagging.

ACKNOWLEDGEMENT

The authors wish to thank the anonymous reviewers for their valuable comments. This work was supported by Malaysia's Ministry of Higher Education Scholarship MyBrain 15 (My Ph.D.) and Bridging Grant, USM (6316122).

REFERENCES

[1] L. Wang, L. D. Xu, Z. Bi, and Y. Xu, "Data cleaning for RFID and WSN integration," *IEEE Transactions on Industrial Informatics*, 10(1), 408-418, 2014.

[2] D. De Donno, L. Catarinucci, and L. Tarricone, "A battery-assisted sensor-enhanced RFID tag enabling heterogeneous wireless sensor networks," *IEEE Sensors Journal*, 14(4): pp. 1048-1055, 2014.

[3] S. Shao, "Design approach for robust UHF RFID tag antennas mounted on a plurality of dielectric surfaces," *IEEE Antennas and Propagation Magazine*, vol. 56, 2014.

[4] M. Attaran, "Critical success factors and challenges of implementing RFID in supply chain management," *Journal of Supply Chain and Operations Management*, vol. 10, no. 1, 2012.

[5] A. Sabbaghi, "Effectiveness and efficiency of RFID technology in supply chain management: Strategic values and challenges," *Journal of Theoretical and Applied Electronic Commerce Research*, vol. 3, issue 2, 2008.

[6] P. C. Jain and K. P. Vijayagopalan, "RFID and wireless sensor networks," *Proceedings of ASCNT, CDAC*, Noida, India, 2010.

[7] L. H. Mei, et al., "Influence of UHF tags in the different material surface to RFID system," *Antennas and Propagation (APCAP), 2014 3rd Asia-Pacific Conference*, IEEE, 2014.

[8] M. N. O'Grady and J. P. Kerry, "Smart packaging technologies and their application in conventional meat packaging systems," in *Meat Biotechnology*, Springer, pp. 425-451, 2008.

[9] I. A. D. Chiara, "Analysis of performance and interferance effects in radio frequency identification systems," 2011.

[10] J. D. Griffin, et al., "RF tag antenna performance on various materials using radio link budgets," *IEEE Antennas and Wireless Propagation Letters*, 5(1): pp. 247-250, 2006.

[11] P. V. Nikitin, K. Rao, and S. Lazar, "An overview of near field UHF RFID," in *RFID*, 2007. *IEEE International Conference on*, 2007, *IEEE*, 2007.

[12] A. Piche, et al., "RFID equivalent model for prediction of functional and EMC performances in complex aeronautic environments," *Aerospace EMC (Aerospace EMC), 2016 ESA Workshop on*, *IEEE*, 2016.

[13] Y. Zhang, et al., "Design of miniaturized UHF RFID tag antenna attached to dielectric and metallic objects," *Antennas and Propagation & USNC/URSI National Radio Science Meeting, 2015 IEEE International Symposium on*, *IEEE*, 2015.

[14] J. Baker-Jarvis, M. D. Janezic, and D. C. Degroot, "High-frequency dielectric measurements," *IEEE Instrumentation & Measurement* Magazine, 2010.

[15] M. Periyasamy and R. Dhanasekaran, "Assessment and analysis of performance of 13.56 MHz passive RFID in metal and liquid environment," In *Communications and Signal Processing (ICCSP), 2014 International Conference on IEEE*, pp. 1122-1125, 2014.

[16] J. Xie, M. Wang, and J. Tan, "A novel method to evaluate the RFID system reliability," *Procedia Engineering*, 174, 465-469, 2017.

[17] A. Sihvola, "Mixing rules with complex dielectric

coefficients," *Subsurface Sensing Technologies and Applications*, (1)4: 393-415, 2000.
[18] L. A. Kosuru, "Optimum performance of UHF RFID tags in dielectric environment," *University of Kansas*, 2011.
[19] J. M. Govardhan, "Performance modeling and design of backscatter RFID systems: A statistical approach," *Oklahoma State University*, 2006.

Renuka Nalinggam obtained her B.S. in Engineering from Universiti Tenaga Nasional in 2005 and her M.Sc. from Universiti Sains Malaysia in 2012. She worked as a Lecturer in the Asian Institute of Medical, Science and Technology University from 2011 to 2012. She currently serves as a Lecturer in Southern University College, Skudai, Johor, while pursuing her Ph.D. in Universiti Sains Malaysia. Her research interests are machine-to-machine communication, radio-frequency identification, and wireless sensor networks.

Widad Ismail is a Professor and Project Coordinator for the Auto-ID Laboratory, Universiti Sains Malaysia. She obtained her B.S. in Engineering (First Class Honors in Electronics and Communication Engineering) from the University of Huddersfield, United Kingdom (1999). She obtained her Ph.D. in 2004 (Active Integrated Antenna with Image Rejection) in Electronics and Communication Engineering from the University of Birmingham, United Kingdom. She worked in the University of Birmingham from 2000 to 2003 as a postgraduate teaching assistant. She has been working as a Lecturer in Universiti Sains Malaysia since 2004. Her areas of research are wireless system design, radio-frequency identification, active integrated antennas, and radio-frequency and microwave systems engineering. She is also a member of the Institute of Electrical and Electronics Engineers and the Wireless World Research Forum.